

ASSESSMENT OF DYNAMIC FRACTURE PROPAGATION RESISTANCE AT INSTRUMENTED HIGH VELOCITY GASGUN IMPACT TESTS ON SENB- SPECIMENS

H. C. van Elst

Metal Research Institute TNO, Apeldoorn, The Netherlands

ABSTRACT

Using as striker a cylindrical high strength steel projectile of 600 mm length and 40 mm diameter (mass 5,8 kg), ejected by a gasgun at velocities up to 80 ms^{-1} , SENB-specimens of 100 mm length, 50 mm thickness and supported on a span of 400 mm were separated by impact.

By suitable instrumentation, using high speed photography, a laser-Doppler technique, a photocell array and straingauges the dissipated energy as a function of crack extension and at separation could be found from energy balance considerations. J_{1c} and $J_R/\Delta a$ curves could be determined as well for the relevant limit load conditions.

KEYWORDS

Dynamic fracture propagation resistance; high velocity impact; gasgun; high speed photography; laser-Doppler technique; electronic instrumentation; straingauges; photocell; energy and momentum balance; energy dissipation; crack velocity; J-integral; limit load and moment; SENB-specimen.

NOMENCLATURE

- x, y, z = Cartesian coördinates of to the laboratory fixed (Euler) OXYZ-system
- O = centre of initial rest position of specimen
- OX = length direction of initial rest position of specimen
- OY = height direction of initial rest position of specimen opposite to crack extension direction in OXYZ
- OZ = thickness direction of (initial rest position) of specimen
- $\underline{x}, \underline{y}, \underline{z}$ = Cartesian coördinates of to the moving specimen half 1 fixed (Lagrange) \underline{OXYZ} -system
- \underline{O} = to a specimen half fixed point, coïnciding with O in the initial rest position
- \underline{OX} = length direction of moving specimen half 1 rotating in right hand way in \underline{YOX} -plane
- \underline{OY} = height direction of moving specimen half 1

OZ	= thickness direction of (moving) specimen half	
t	= time	[s]
l	= length of specimen half	[m]
$2l-2q$	= span of specimen	[m]
w	= height (or width) of specimen	[m]
b	= thickness of specimen	[m]
D	= diameter supports	[m]
m	= mass of specimen half	[kg]
s	= density of specimen material	[kg m ⁻³]
a	= cracklength	[m]
T	= moment of inertia of specimen half w.r.t. axis in thickness direction through its centre of gravity	[kg m ²]
ϕ	= rotation angle	
ρ	= rotation factor	[kg]
M	= mass of projectile	[ms ⁻¹]
V	= projectile velocity (in OXYZ-system)	[m]
r	= polar radius	[kg ms ⁻¹]
p	= momentum	[N]
v	= velocity in surface point of impacted specimen	[s]
ρ	= rotation factor = $(a_e - a)/(w - a)$	[m]
P	= force	[mN]
τ	= impact duration	[J]
f	= deflection	[MNm ⁻²]
δ	= crack mouth edges distance	[Nm ⁻¹]
CTOD	= crack tip opening displacement	[m]
C	= elastic compliance	[mN ⁻¹]
E	= energy	[J]
E	= Young's modulus	[MNm ⁻²]
R	= fracture resistance	[Nm ⁻¹]
Y	= yield strength	[MNm ⁻²]
Q	= applied moment	[Nm]
I	= area moment of inertia of cross section	[m ⁴]
c	= sound velocity	[ms ⁻¹]
γ	= correlation coefficient for curve fitting	
J	= J-integral	[MNm ⁻¹]
λ	= a/w	

subscript: to: refers to:

1,2	1,m,T,p,Z,v	specimen half 1,2
o	a,V, δ	initial value
i	t, ϕ , ρ ,a	moment of impact of specimen and supports
e	a	elastic equivalent
Z	x,r	centre of gravity
P	τ ,P	projectile and specimen
s	τ ,P	support(s) and specimen (half)
kin	E	kinetic energy
transl	E	translational kinetic energy
vib	E	vibrational kinetic energy
rot	E	rotational kinetic energy
elast	E	elastic energy
diss	E	dissipated energy
diss; p	E	dissipated energy for ligament zero (dissipated energy due to penetration of projectile into specimen)
diss; a	E	dissipated energy by crack extension
lim	ϕ ,Q,P	limit load or moment conditions
Y	r	plastic zone size at crack tip

superscript to: refers to:

sep	E	at complete specimen separation
*	a	notional cracklength ($a^* = a + r_Y$)

abbreviations: SENB, single edge notch bend; h.s.p.(r.), high speed photography (recordings)

INTRODUCTION

In a previous paper (Van Elst, 1981a) the evaluation of the fracture propagation resistance from impact testing of SENB ("dropweight tear test like") specimens, using a projectile ejected by a gasgun as striker and applying suitable instrumentation was described. The same experimental technique was applied in this investigation while moreover a laser-Doppler technique was used in addition to record two (displacement) velocities in x- and y-direction or both in x-direction at the specimen surface in two (sometimes one) fixed laboratory system positions (position) resp., situated at the surface of a specimen half in its original rest state. This appeared more promising for assessment of the kinetic energy of the impacted specimen required for the envisaged energy balance analysis than the (previously applied time consuming) method, in which the angular velocity had to be deduced from the with high speed photography recorded angles of rotation in time of the specimen, in order to find its (rotational) kinetic energy. High speed photography was applied as before to record the crack extension. On the determination of the kinetic energy in time of the impacted specimen from the laser-Doppler technique recordings is elaborated below and in Van Elst (1984).

MATERIAL AND SPECIMENS; TEST KINEMATICS

50 mm thickness steelplates of a low alloy structural steel Fe510 (code 659K), conforming to B.S. 1501-281 A and a 5% Ni structural steel HY130 were investigated as to their dynamic fracture propagation resistance. Drop weight tear test like SENB-specimens from both available steelplates were prepared with 100 mm width, 50 mm thickness (cf. Fig. 1) and 450 mm length for the Fe510 steel and 440 mm length for the HY130 steel resp.; the

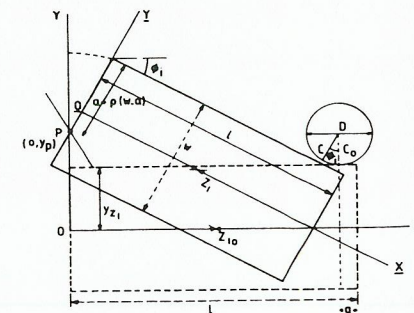
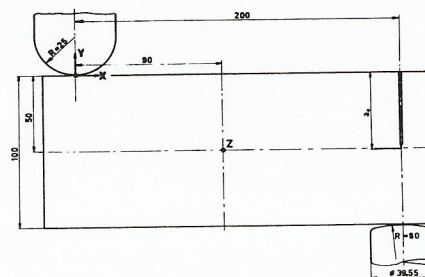


Fig. 1. SENB impact specimen, striker Fig. 2. Kinematic topography of impacted SENB specimen

¹ Situation is drawn, where impacted specimen - after having lost initial contact with striker and supports - hits the latter again.

span was 400 mm. The Fe510 steel plate specimens were provided with a fatigued notch tip. The HY130 steel plate specimens had a machined notch with 0.3 mm (at the tip). The geometry and dimensions of the for impact testing used striker (a cylindrical projectile ejected by a gasgun at velocities up to 80 m s⁻¹) and those of the specimens are shown in Fig. 1. The topography of the impacted specimen is illustrated in Fig. 2; on its kinematics is elaborated elsewhere (Van Elst, 1981a, 1984).

EXPERIMENTAL METHODS; DATA STORAGE AND PROCESSING

Recordings in time of the angular velocity and angle rotation and of the displacements in x- en y-direction of the centre of gravity of a specimen half, using a laser-Doppler technique.

Scotch lite tape, type 3290 white, was glued onto the specimen surface to facilitate the observations. For storage of the v_1 and v_2 values with 5 μ s intervals were (one) Biomation 8100 and (four) Biomation 805 transient recorders at disposal. The first one functions as "master" and triggers the other ones; it was externally triggered by an impact signal ("breaking wire") of projectile and specimen. The output of the strain gauges responses on the supports was recorded in intervals of 5 μ s by parallel channels (1 and 2) of the (Biomation 8100) transient recorder. Parallel channels 5 up to 6 of the (Biomation 805) transient recorders were used for the (v_1, v_2) recordings, applying the same time clock (set by crystal resonance frequency and providing the 5 μ s interval signal storage.) The applied high speed camera was a moving film Hycam camera, model K20 S4W, provided with a rotating prism unit K20 HW and sectors shutter 1:5. This allows to record 10⁴ f.p.s. with an illumination time of 1/5 x 10⁻⁴ sec. The objective was from Schneider with focal distance 3.5 mm; opening 1:2; applied was diafragma 8. Kodak Plus X 16 mm film with image dimensions 10 x 8 mm was used. Illumination proceeded in a continuous way by 6 halogen bulbs with reflectors (each bulb 36V - 340 watt.), which cast light on the specimen under 45°. The specimen was sprayed with "anti-reflex". The camera was used to trigger the electrical valve of the gasgun, which admits the compressed air in the barrel for driving out the projectile. The camera gives an opening signal to this valve ca. 0.1 sec. after start of the film rotation, which causes the projectile to hit the specimen some 500 ms later (of which ca. 100 ms are used for travel through the barrel of the projectile). At that time the rotating film speed of the camera (\approx 100 m/sec.) has become rather constant (this occurs after 70 to 100 m film is being spent). The pictures shot after this period start to show the projectile. From the velocity of the projectile - which is known from these pictures and also from the response of an illuminated photocell array onto which the passing projectile casts its shadow, (cf. Van Elst, 1981a, 1984) - and its distance to the specimen, the time at which the relevant pictures is shot, is known. As light pulses with intervals of 1 ms are recorded on the film as well, the time clock of the film can thus be linked to that of the transient recorders. This allows to indicate the cracklength in the "read-out" of the transient recorders, which was processed with intervals of 50 μ s for y_1 and y_2 , the ordinates (in striker direction) of the fixed laboratory positions, where v_1 and v_2 were observed. With intervals of 25 μ s the strain gauges responses P_1 and P_2 of the forces on supports 1 and 2 resp. were read. These data allow to find the possible change of (translational) momentum of specimen in striker direction, the velocity in x-direction of the centre of gravity of a specimen half, its angular velocity (as elaborated in Van Elst, 1984) and the synchronous value of the cracklength. The velocities V_0 and V of the projectile with mass M , just before and

after impact with the specimen, measured with the photocell array are stored in the Biomation 850C transient recorder with 5 μ s sampling time as well; these velocities could be compared with those deduced from the high speed photographic recordings. A manual calculator (Hewlett and Packard 97), which could be considered adequate for the data processing, was used.

It was assumed that the momentum transfer from projectile to specimen proceeded linearly in time and was accomplished in 250 μ s (Van Elst, 1984).

[This in fact appears somewhat better justified, if the specimen dimensions in striker direction being 100 mm) would have been larger than the projectile length (being 600 mm) and the cross section of projectile and specimen rather the same. For such a latter situation an (elastic) approximation of

the transferred rectangular pulse time is $\tau = 2L/c = \frac{2 \times 600 \text{ mm}}{5 \text{ mm}/\mu\text{s}} = 240 \mu\text{s}$ with

L = projectile length and c = sound velocity. The applied force $P_T/\tau \approx \frac{1}{2}sc(V_0 - V)$ with s = specific mass of specimen material is then constant for $P_T = M(V_0 - V)$ = totally transferred momentum by projectile in time $2L/c$. As during the first 250 μ s no loss of contact was observed between projectile and specimen in the high speed photographic recordings of the performed tests, the mentioned assumption appears a fair approximation.]

RESULTS

The evaluation of $\frac{1}{2}m\dot{y}_{Z1}^2$, $\frac{1}{2}m\dot{x}_{Z1}^2$, $\frac{1}{2}I\dot{\phi}^2$ and ϕ for a specimen half at successfully performed tests proceeded with a manual calculator, using relevant algorithms as developed in Van Elst (1984). The observed velocities in (x_1, y_1) and (x_2, y_2) and the calculated data outputs of ϕ , \dot{y}_{Z1} , \dot{y}_{Z1} , \dot{x}_{Z1} , x_{Z1} are given in loc. cit. (and in a there referred report, which can be obtained on request). From the experiment on a specimen with 1 mm wide, i.e. nearly through initial ligament an estimate of the dissipated energy $E_{diss;p}$ by projectile penetration into the specimen only could be made. This latter energy dissipation presumably is completed before crack extension starts for finite ligament specimen. To find the energy dissipation $E_{diss;a}$ at crack extension the total energy dissipation $E_{diss} = \frac{1}{2}M(V_0^2 - V^2) - E_{kin}$ has to be decreased with the $E_{diss;p}$. From an experiment with initial ligament nearly zero was estimated $E_{diss;p} = 6.5 \text{ kJ}$ (however, cf. DISCUSSION). In Fig. 3 the totally dissipated energy for specimen separation E_{diss}^{dep} was plotted versus initial ligament ("multiple specimens approach"). Also $(E_{diss}^{dep} - E_{diss;p})/b(w-a_0)$ was plotted versus $w-a_0$; this shows the anticipated linear behaviour (cf. loc. cit. and DISCUSSION). The dissipated energy $\frac{1}{2}M(V_0^2 - V^2) - E_{kin} - E_{diss;p}$ and the cracklength a were plotted as functions of time. An example is shown in Fig. 4. From such diagrams also the diagrams of dissipated energy versus cracklength were plotted for the single test pieces; cf. DISCUSSION.

ANALYSIS OF EXPERIMENTAL RESULTS

A rather large scatter of the E_{kin} -evaluations in time, also in its parts: $E_{transl} = 2 \times \frac{1}{2}m\dot{y}_{Z1}^2$; $E_{vib} = 2 \times \frac{1}{2}m\dot{x}_{Z1}^2$ and $E_{rot} = 2 \times \frac{1}{2}I\dot{\phi}^2$, proved present. This is probably due to the non equilibrium stress configuration at each moment in the impacted tearing specimen. This will deviate from the static one for a certain deflection not only by (possible) stress amplitude (increase) due to dynamic effects, but also by the presence of running stress waves. The laser-Doppler technique measures the therefore relevant displacement velocities at the specimen surface. However when the movement of the specimen is very fast (as in the experiments on specimens with

practically zero ligament) the available laser-Doppler technique equipment can obviously not follow, when the acceleration is too fast. A frequency of 40 kHz per ms⁻¹ is observed by this equipment; cf. Oldengarn (1976, 1977). The maximum frequency change per unit time that can be observed is 5 MHz per millisecond.

This implies, that accelerations up to $1.25 \times 10^5 \text{ ms}^{-2} \approx 12500 \text{ g}$ can be followed. If a particle velocity of $\dot{u} = 25 \text{ ms}^{-1}$, corresponding with an (elastic) stress of $\sigma_{cu} = 8 \times 10^3 \times 5 \times 10^3 \times 25 \text{ Nm}^{-2} = 1000 \text{ MNm}^{-2}$ is achieved in 10 μs , the acceleration is of the order $25 \times 10^5 \text{ ms}^{-2}$, which is 20 x larger. Running stress waves can thus imply errors of velocity recordings in time, while moreover the geometrical link between velocities in different points as elaborated in Van Elst (1984) can be violated. The applied interpretation of the velocities as recorded by the laser-Doppler technique can then be at fault. Also a non symmetrical division of the specimen by the moving crack will entail unequal distribution of kinetic energies in both specimen halves; as only one specimen half was observed this too account for scatter. [An analytical estimate of the kinetic energy obtained by a specimen with zero ligament can in principle be given as well. For this a specimen with zero ligament, but with an ideal hinge at the point of impact, operative after impact as long as it experiences compressive forces and then moving in striker direction can be considered. The relevant differential equations describing the movement of such a specimen are given in Van Elst (1984). These equations suggest that the rotational movement has a harmonic character with a damping proportional to ϕ^2 ; it might account for the oscillatory appearance of $\frac{1}{2}T\dot{\phi}^2$ as calculated; a frequency estimate has not yet been made.] The totally dissipated energies E_{diss}^{sep} for separation of the specimens:

$E_{diss}^{sep} = \frac{1}{2}m(V_0^2 - V^2) - E_{kin}^{sep}$, plotted versus $(w-a_0)$ in Fig. 3 (cf. RESULTS), were curve fitted according to:

$$E_{diss;a}^{sep} = E_{diss}^{sep} - E_{diss;p} = \bar{R}b(w-a_0) + \bar{S}b(w-a_0)^2 \quad (1)$$

with presumably \bar{R} = average fracture resistance with the dimension (MNm⁻¹) of an effective surface energy and \bar{S} = effective energy density with the dimensions [MNm⁻²]. Such a description was found adequate in tearing experiment on notched specimens of other (ductile) steels (in particular line pipe steel), when a completely yielding ligament occurs (Van Elst, 1981b). \bar{R} refers to the local plastic work in the so called process zone near the crack tip; while \bar{S} refers to remote global plastic work unavoidably accompanying the tearing. As figures were obtained:

$$E_{diss;p} = 3.90 \text{ kJ}; \bar{R} = 1.18 \text{ MNm}^{-1}; \bar{S} = 21.6 \text{ MNm}^{-2}; \gamma^2 = 0.894.$$

In this description the dissipated energy value estimated from the experiment with nearly through ligament was rejected, as this would have implied a minimum energy dissipation for finite ligament (and a negative value of \bar{R}). However from the model with zero ligament as analysed (Van Elst, 1984) a satisfactory value for this dissipated energy was found, viz. 4.1 kJ. Using the assumption that the momentum transfer from projectile to specimen during impact linearly proceeds in time (loc.cit), the kinetic energy shows a monotonic ("smooth") increase. Crack extension starts at about the time that this momentum transfer has been completed (presumably after ca. 250 μs). From this onwards the kinetic energy as deduced from the velocity recordings with the laser-Doppler technique shows an oscillatory behaviour. Consequently the anticipated decrease of kinetic energy when the crack extends is not easily detected and in fact it even seems sometimes absent. Decreasing the loss of kinetic energy of the projectile with both the obtained kinetic energy of the specimen and with the dissipated energy by projectile penetration into the specimen offers E_{diss}^a . This was plotted versus time. Cf. RESULTS. On the same time axis the cracklength a is plotted. This

allows to find the diagram of $E_{diss;a}$ versus a (in which the oscillatory behaviour of the kinetic energy of the specimen effectuates less disturbance); Fig. 4 shows an example. The estimate of the slope in a relevant a -interval, usually (a_0, w) in this latter diagram offers a R -value, indicated as \bar{R} . A (systematic) error in $E_{diss;p}$ will not influence

$R = \frac{dE_{diss;a}}{da}$ or its approximation \bar{R} . [The intermittent drawn part of the curve $E_{diss;a}$ in the time interval (0-150 μs) was obtained by assuming that the kinetic energy loss of the projectile and energy dissipation by projectile penetration into the specimen linearly proceeded in time. A possible physical meaning of this $E_{diss;a}$ before crack extension starts might be attributed to a dissipation of energy required for crack initiation.]

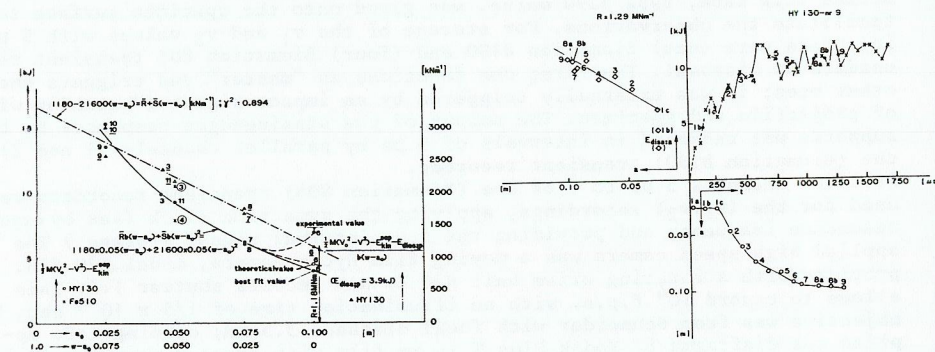


Fig. 3. Dissipated energy and average dissipated energy per unit crack area increase at separation of impacted SENB-specimens versus initial crack size

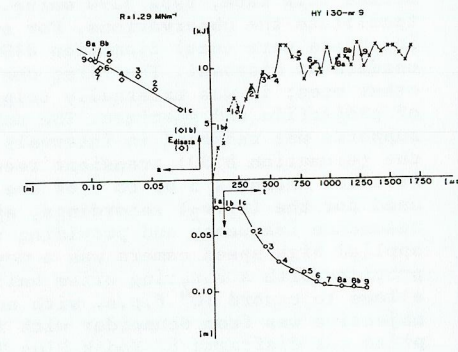


Fig. 4. Dissipated energy and crack length versus time and dissipated energy versus cracklength during tearing of impacted SENB-specimens (HY130-9; $a_0 = 25 \text{ mm}$)

J AND R INTERPRETATION OF RESULTS FROM LIMIT CONDITIONS

Though for the dynamic non equilibrium situation the J-integral is path dependent, yet a quasi-static J-integral evaluation was explored. As load data causing specimen deflection are not (directly) observable - in fact deflection and tearing proceed, when the specimen is free from external loads or moment after impact - an expression for J in the observable ϕ is required. Assumedly the beyond limit load situation is realized already at initiation and using the relevant expression for 3 points SENB-specimens for this (cf. e.g. Rice, Paris and Merkle, 1973), one derives with Q referring to the moment part causing deformation only:

$$J = \frac{Q\phi_{crack}}{b(w-a)} \left\{ 2 - \frac{(\phi_{crack})_{lim}}{\phi_{crack}} (1-16\beta D_2^2) \right\} \quad (2.1)$$

$$= D_2 \bar{Y} w (1-\lambda) \phi_{\text{crack}} \left\{ 2 - \frac{(\phi_{\text{crack}})_{\text{lim}}}{\phi_{\text{crack}}} (1-16\beta_2^2) \right\} \quad (2.2)$$

ϕ_{crack} = rotation angle, due to the crack; \bar{Y} = effective yield strength
 $D_2 = 0.36$; cf. Green and Hundy (1956); $\beta = \frac{1}{2\pi}$ for the assumedly relevant plane stress situation; $16\beta D_2^2 = 0.35$ and can become up to 3 x smaller, when plane strain is prevailing. For $(\phi_{\text{crack}})_{\text{lim}}$ was taken ϕ at 250 μ s; at this time initiation (usually) starts and the limit load situation is arrived at.

In Fig. 5 thus evaluated J-values are presented. No correction for strain hardening was attempted, which unfavorably interferes with tearing modulus estimates from J/ Δa -curves; cf. also Rice, Paris and Merkle (1973) and Wilson (1970). To account for the absorbed energy during crack extension in SENB-specimens under limit load conditions one has with:

$$P_{\text{lim}}(\lambda) = \frac{4}{3} \bar{Y} b (w-a)^2 / 2\ell = \frac{4}{3} \bar{Y} b w^2 (1-\lambda)^2 / 2\ell \quad (3)$$

and thus for span $2\ell = 4w$ as relevant: $P_{\text{lim}} = \frac{1}{3} \bar{Y} b w (1-\lambda)^2$

$$E(\lambda, \lambda_0) = \frac{1}{3} \bar{Y} b w \int_{\lambda_0}^{\lambda} (1-\lambda)^2 d\lambda = \frac{1}{3} \bar{Y} b w^2 \int_{\lambda_0}^{\lambda} (1-\lambda)^2 \frac{\dot{\lambda}}{\dot{a}} d\lambda = \frac{1}{9} \bar{Y} b w^2 \frac{\dot{\lambda}}{\dot{a}} \{ (1-\lambda_0)^3 - (1-\lambda)^3 \} \quad (4)$$

$$E_{\text{diss}}^{\text{sep}}(\lambda, \lambda_0) = \lim_{\lambda \rightarrow 1} E(\lambda, \lambda_0) = \frac{1}{9} \bar{Y} b w^2 \frac{\dot{\lambda}}{\dot{a}} (1-\lambda_0)^3 \quad (5)$$

With $\bar{Y} = 900 \text{ MNm}^{-2}$; $b = 0.05 \text{ m}$; $w = 0.1 \text{ m}$ and - according to observation - $\dot{\lambda} \approx \dot{\gamma}_{Z_1} = 25 \text{ ms}^{-1}$; $\dot{a} = 100 \text{ ms}^{-1}$; $\frac{1}{9} \bar{Y} b w^2 \frac{\dot{\lambda}}{\dot{a}} = 0.0125 \text{ MNm}$, (5) appears to offer

a rather satisfactory description of $E_{\text{diss}}^{\text{sep}} - E_{\text{diss;p}}$, while (4) describes $\frac{1}{2} M (V_0^2 - V^2) - E_{\text{kin}} - E_{\text{diss;p}}$; cf. Fig. 3 and Fig. 4 and Fig. 6.

$$R(\lambda) = \frac{1}{b w} \frac{dE}{d\lambda}(\lambda, \lambda_0) = \frac{P_{\text{lim}}(\lambda)}{b} \frac{\dot{\lambda}}{\dot{a}} = 7.5 (1-\lambda)^2 \text{ MNm}^{-1} \text{ and } \hat{R} = \frac{1}{9} \bar{Y} w \frac{\dot{\lambda}}{\dot{a}} (1-\lambda_0)^2.$$

CONCLUSIONS

Displacement controlled impact tests on SENB-specimens, in which contact between striker and specimen and supports and specimen is lost, yet allow estimates of J_{1c} , J/ Δa -curve and dissipated energy $E(a)$ by suitable recordings of displacement, velocity, angular velocity and cracklength in time.

In the investigated upper shelf level, where presumably ductility dictates limit (dynamic) moment conditions, J-values appear to remain ligament dependent, while the dissipated energy for crack extension appears to be describable as:

$E_{\text{diss}}(\lambda, \lambda_0) = \frac{1}{9} \{ \bar{Y} b w^2 \frac{\dot{\lambda}}{\dot{a}} \} \Gamma(\lambda)$, with \bar{Y} a yield strength value for relevant strainhardening and deformation rate and $\Gamma(\lambda)$ a geometrical factor as described in (4) and for $\lambda = w$ in (5) resp.

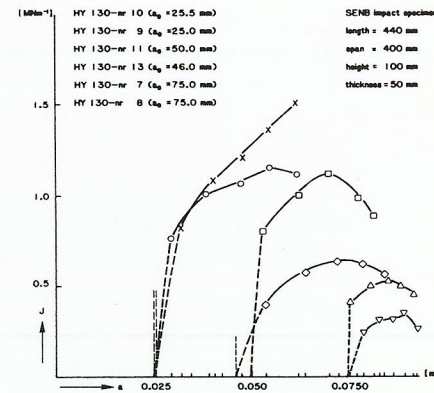


Fig. 5. J/ Δa -curves for impacted HY130-steel SENB-specimens (with a_0 as parameter)

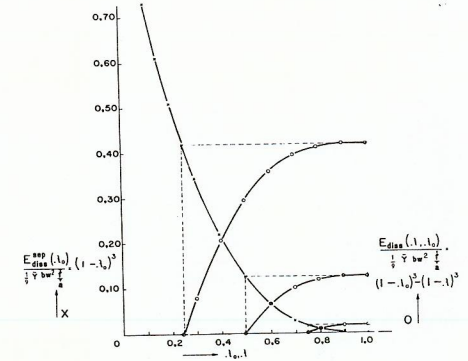


Fig. 6. Normalised dissipated energy at crack extension and separation for impacted HY130-steel SENB as function of λ and λ_0 resp. under limit moment conditions

NOTE

For more quantitative details, examples of high speed photographic recordings, fracture surface appearances, etc. is referred to Van Elst (1984).

ACKNOWLEDGEMENT

The larger part of this work was made possible by contract N68171-82-C-9517 with U.S.-Navy, to which our thanks are due for permission to publish this paper. The experimental work proceeded under guidance of Mr. Lont.

REFERENCES

- Elst, H.C. van (1981). Proc. of the 5th Int. Conf. on Fracture, ICF5, Cannes, France, 2, 1059-1072 (editor D. François at Pergamon Press).
- Elst, H.C. van (1984). Proc. of the 5th Eur. Conf. on Fracture, ECF5, Lissabon, Portugal (to be edited by L. Faria).
- Elst, H.C. van (1981). Proc. of the 4th AGA-EPFG Linepipe Research Seminar, 1-nr. 7 (edited by G. Vogt at Mannesmann Forschungsinstitut, Duisburg, W-Germany).
- Green, A.P. and B.B. Hundy (1956). J. of Mech. and Phys. of Sol. 4, 128-144.
- Oldengarn, J. and Prabha Venkatesh (1976). J. Phys. E. Sci. Instr. 9, 1009-1012.
- Oldengarn, J. (1977). Opt. and Laser Techn. 9, 69-71.
- Rice, J.R., P.C. Paris and J.G. Merkle (1973). Progress in flaw growth and fracture toughness testing. ASTM-STP 536, 231-245.
- Wilson, W.K. (1970). J. of Eng. Fracture Mech. 2 nr. 2, 169-171.